Filter design and applications in image improvement

T. Mongy*, Montaser Tharwat Alaaeldin

Egyptian Atomic Energy Authority (EAEA), ETRR-2, 13759, Egypt.

*Email:tmongy@gmail.com

Abstract:

This work presents the performance analysis of different basic techniques used for the image restoration. Restoration is a process by which an image suffering from degradation can be recovered to its original form. Removing the noise from the image is the scope of this work. The work implemented different techniques of image enhancement and noise removal. The degraded images have been restored by the use of different mathematical filters.

A new approach using MATLAB software was designed to improve the image and suppress the noise. The code was executed to eliminate the image degradation and avoid the loss of information. The use of the code enables easy extraction of data from the images.

Keywords: MATLAB code; Neutron imaging; Filter design.

1. Introduction:

The goal of image denoising methods is to recover the original image from a noisy measurement [1-3]. The goal of filtering is to eliminate as much noise and retain as much signal as possible. Some image filters were used to remove imperfections [4]. The use of denoising algorithms can handle with non-homogenous noise [5]. Most of filters are characterized by cut-off frequency and order parameters. The cut-off frequency defines the frequency from which higher frequencies will be suppressed and therefore denotes the bandwidth of the filter. The amplitude of the filter at the cut-off frequency is dependent on the type of the filter, such as Butterworth and Gaussian. The filters are defined by a second parameter, the order of the filter. This parameter tunes the filter by changing the slope of the filter function and allows the user to optimize the tradeoff smoothness– sharpness of the image [6-7].

This work presents mathematical techniques for high quality neutron tomography (NT) images. The techniques were based on applying low-pass imaging filters for removing high frequencies. Low-pass filter, Gaussian filter and Butterworth filter were used for image improvement. Additionally, this work presented a new technique for imaging processing. A new model was executed to reduce error and suppress noise; this method was designed to improve the image contrast image quality.

2. Neutron Radiography Facility:

All activities performed within the frame of this work have been performed at the neutron radiography facility (NRF). An overview of the main characteristics of this facility is given Table (1).

Table 1. The main characteristics of the NRF.

Parameter	Value
Reactor nominal power (MW)	22
Neutron flux density [$n.cm^{-2}s^{-1}$]	~$1.5*10^{7}$
L/D ratio	117.3
Cadmium (Cd) ratio	10.26
Beam outlet diameter [cm]	20
γ-background at the full power [Sv/h]	5.5
strength of the neutron source [n/s]	$28*10^{8}$

Fig. 1 represents the geometric model of the NRF. It comprises from:

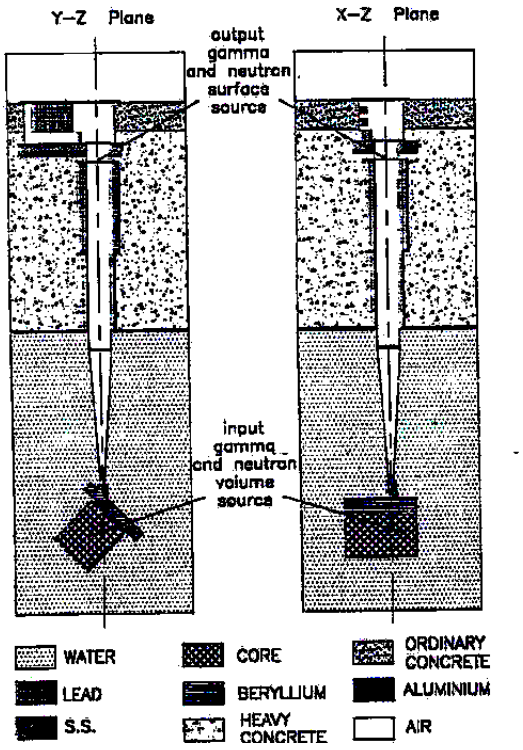

Fig.1. Geometric model of the NRF.

1- Reactor core as a stationary planar neutron source,

2- Gamma ray lead filter to reduce gamma intensity emerged with the neutrons,

3- Divergent aluminum collimator, submerged into the water of the reactor tank. The collimator is internally lined by 2 mm thickness cadmium (Cd) sheet. The function of the collimator is to collimate thermal neutrons,

4- The irradiation conduit. It is cut cross the biological shield and internally lined with 2 mm Cd sheet, its function is to contribute with the collimator to get well defined beam,

5- The lead beam shutter.

2.1 Neutron imaging (NI) system:

Digitization of the NRF has the potential to improve the performance of the neutron radiographic investigations. A high-resolution, 14-bit charged-coupled device (CCD) [8] cooled camera system, was installed recently at the NRF. This camera exhibits a superior resolution with advanced thermo-electrical technology in CCD ships cooling. Table (2) highlights the main parameters of the CCD-camera.

Table 2. Main parameters of the CCD-camera.

Parameter	**Value**
Pixel array format (horizontal x vertical) pixel	2048*2048
Sensitive Area [mm]	200 x 200
Pixel Size [μm^2]	7.4 x 7.4
Digitization (Dynamic Range)	14 bit (32768 gray levels)
Dark current (e^-/pixel.s)	0.5
Image Frame Rate (Frame/Sec.)	14.7
Exposure Time	5 µsec. to 49 days
Data interface	IEEE1394a
Cooling Method	Peltier cooler to -50 degree versus ambient temperature

2.2 The degradation model:

The simple equation for expressing image degradation is as follows [9];

$$g(x,y) = h(x,y) * f(x,y) + \eta(x,y) \quad (1)$$

where:

f(x,y) is the original image or true image estimation,
g(x,y) is the version that has been degraded through noise (convoled $*$) by kernel *h* and
η(x,y) is the additional random noise or error.

Consider:

$$f(x,y) * h(x,y) = g^-(x,y) \quad (2)$$

where:

$g^-(x,y)$ is the deviated image from the original one *f(x,y).*

From the definition of the deconvolution, it is an algorithm-based process used to reverse the effects of convolution on the recorded data [8], then the restored image *f(x,y)* can be modeled as:

$$f(x,y) = D^{-1}(g\text{-}(x,y) * h(x,y)) \quad (3)$$

where:

$\boldsymbol{D^{-1}}$ is the deconvolution operator.

From equation (1), the improved image ***f(x,y)*** can be expressed as:

$$f(x,y) = D^{-1}((g(x,y) - \eta(x,y)) * h(x,y)) \quad (4)$$

Fig. 2 shows a model of the image degradation process.

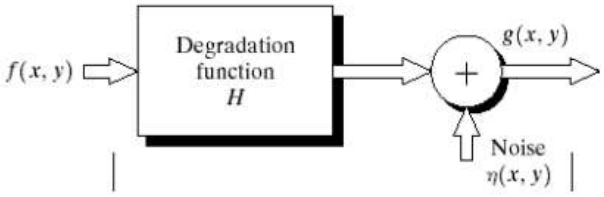

Fig. 2. Image degradation model.

Fig. 3 and 4 show the noisy neutron tomography (NT) images of a thyme plant and a CV car joint, respectively. The unprocessed noisy images show low quality images; therefore, mathematical image processing technique was executed.

Fig. 3. NT of a thyme plant.

Fig. 4. NT of a CV car joint. The noise is clear at the top part of the image.

3. Previous work:

Reference [11] introduced a new iterative procedure for significant improvement of digital images by solving the variational problem of Rudin-Osher-Fatemi (ROF) model. The main results in this work concerned an iterative regularization procedure designed to improve ROF restoration and its generalizations. The solution was computed by using Bregman distance algorithm. The novel idea is to replace the ROF problem by a sequence improved designed algorithm; so as to obtain an improved restoration.

Reference [12] used different kinds of filters for noise reduction; such as, linear filters and non-linear filters. The problem with some linear filters is that it blurs the edges and details in an image and it is not effective for impulse noise (salt-and-pepper). On other side, some non-linear filters; such as, median filter, is very effective in removing salt and pepper or impulsive noise while preserving image detail.

Reference [13] demonstrated a state-of-the-art algorithm grayscale image denoising by adapting the orthogonal matching pursuit (OMP) algorithm. The technique describes an extension of the denoising algorithm to the proper handling of nonhomogeneous noise. The development is crucial in the cases of missing values. Treating the missing values, as corrupted, was accomplished by a strong impulse noise. The general solution setting fits the problem. The solution demonstrated successful proposed scheme in denoising applications.

F. Edward described all kinds of noise and their solution in computer tomography (CT) [14]. He put modern techniques for artifact reduction. To enable noise reduction, iterative reconstruction technique was used. The iterative methods [15, 16] use a statistical model of the noise to improve the image on each iteration, this enables higher resolution scans and smooth images as well.

4. Explanation of imaging degradation:

The 2D Gaussian function $G(x,y)$ is defined as [17]:

$$G(x,y) = \frac{1}{2\pi\sigma^2} \exp\left(-\frac{x^2+y^2}{2\sigma^2}\right) \quad (5)$$

where

σ is the standard deviation and gives the width of the Gaussian bell curve, and ***x***, ***y*** are the Cartesian coordinates.

The Gaussian smoothing filter function can be written as:

$$G(x,y) = e^{-\frac{x^2+y^2}{2\sigma^2}} \quad (6)$$

The Gaussian function exhibited a property that was particularly useful for this model. This property indicated that the Gaussian smoothing filter was an effective low-pass filter, i.e., the filter that passes signals with a frequency lower than a certain cut-off frequency and attenuates signals with frequencies higher than the cut-off frequency. The width, and hence the degree of smoothing (σ) or the cut-off frequency (f_c) values, were taken to be 0.39, 0.43 and 0.45. The output images of the code are shown in Fig. 5. The figure shows that the image became enhanced by reducing the high frequency noise at f_c equal to 0.45, resulting in sharp edges.

Fig. 5. Processed image by Gaussian low-pass filter with different f_c values.

The change of f_c executed an optimal tradeoff between filtering and noise smoothing; it removed the additive noise and based on stochastic framework. The restored image is improved in terms of the visual performance [18], rather than mathematical measurements. The same filter was applied on the CV car joint image with different f_c values, the results are shown in Fig. 6.

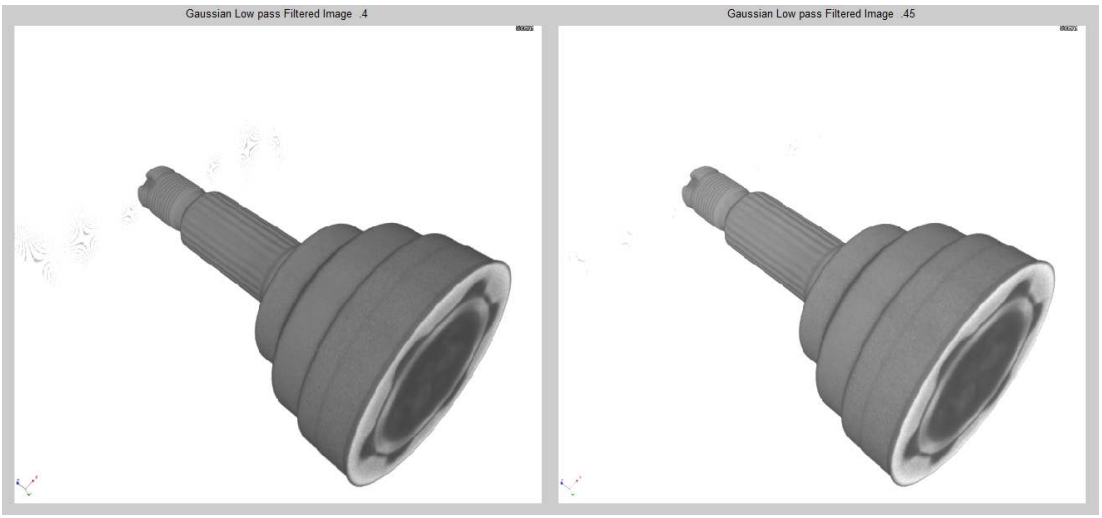

Fig. 6. Processed image of the CV car joint tomography image by Gaussian low-pass filter with different f_c values.

The high-quality image with maximum noise suppression has been accomplished with f_c equal to 0.45.

4.1 Image smoothing by low-pass filter:

Low-pass filter or smoothing filter [19] was employed to remove high frequencies and reduce the noise from the image. The low-pass filter is:

$$d=x^2+y^2 \tag{7}$$

$$y(x,y)=I(x,y)/(I(x,y)+((d/f_c)^{(2*n)})) \tag{8}$$

where:

x, y are the Cartesian coordinates.
$y(x,y)$ is the modified image and
$I(x,y)$ is the original image,

The code was executed with different f_c, the order of the filter (n) was taken to be one. The change of n value darkens the image. The resultant images are shown in Fig. 7 with f_c equal to 0.45, 0.5 and 0.55. The same filter was used for the CV car joint image. The best image is shown in Fig. 8 with f_c = 0.55.

Fig. 7. Processed image by low-pass filter with different cut-off frequencies. The suppression of the noise is pronounced with f_c= 0.50.

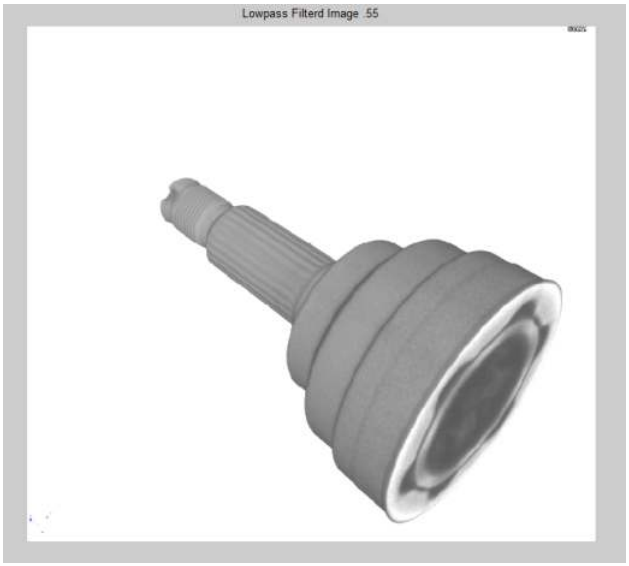

Fig. 8. Smoothing low-pass filter of CV car joint. The suppression of noise is pronounced with f_c= 0.55.

4.2 Imaging denoising by modified Butterworth filter:

The n^{th} modified Butterworth low-pass filter is given by:

$$B(x,y) = \frac{1}{\sqrt{1+[(x^2+y^2)/f_c]^{2n}}} \tag{9}$$

The most appropriate value of n is 1. The advantage of this modified filter is that it does not exhibit a sharp discontinuity. The modified filter may be viewed as a transition between the two extremes of the ideal filter and the Gaussian filter. The definition of the cut-off frequency (f_c) is the main drawback of this filter.

The MATLAB code was executed for different f_c. (0.22, 0.2 and 0.19), the output images are shown in Fig. 9.

Fig. 9. Processed image by modified Butterworth low-pass filter with different f_c values.

The code was executed for different f_c. (0.1, 0.2 and 0.25) for the CV car joint image, the output images are shown in Fig. 10.

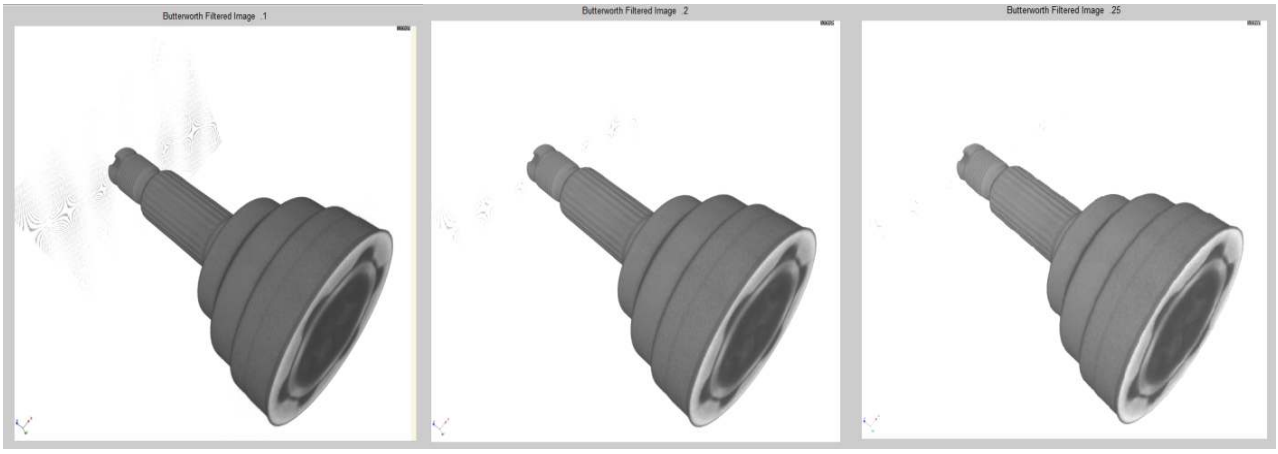

Fig. 10. Processed image by modified Butterworth low-pass filter with different f_c values.

4.3 Improving image quality by reducing the level of error (iterative model):

The novelty of this work consists of executing a new code for noise depression based on Eq. (1). This method was designed to improve the image contrast and reduce the level of errors.

The model proposed that the original unprocessed NT image $g(x,y)$ can be represented as two images; the direct required image $f(x,y)$ or tomographic image that does not have any errors, convolved with the blurred image $\bar{g}(x,y)$ by the electronic components of the NR/T system, in addition to random noise or errors $\eta(x,y)$.

According to Eq. (1), the error $\eta(x,y)$ results from subtraction of the degraded NT image $g(x,y)$ and the deconvolved blind image $f(x,y)$. Since the degradation of the image is unknown, the iterative technique was used to improve the image and reduce the factor of errors. The iterative method was executed to produce a sequence of images by subtracting the resultant error $\eta(x,y)$ from the degraded NT image $g(x,y)$.

The module can be mathematically expressed as:

$$\eta(x,y) = g(x,y) - f(x,y) \tag{10}$$

$$f(x,y) = g(x,y) - \eta(x,y) \tag{11}$$

The results are shown in Fig. 11. The module exhibits better performance for noise depression. The resultant image provided image improvement after three iterations, more features in the root part appeared. Fig. 12 shows the flowchart of the iterative technique.

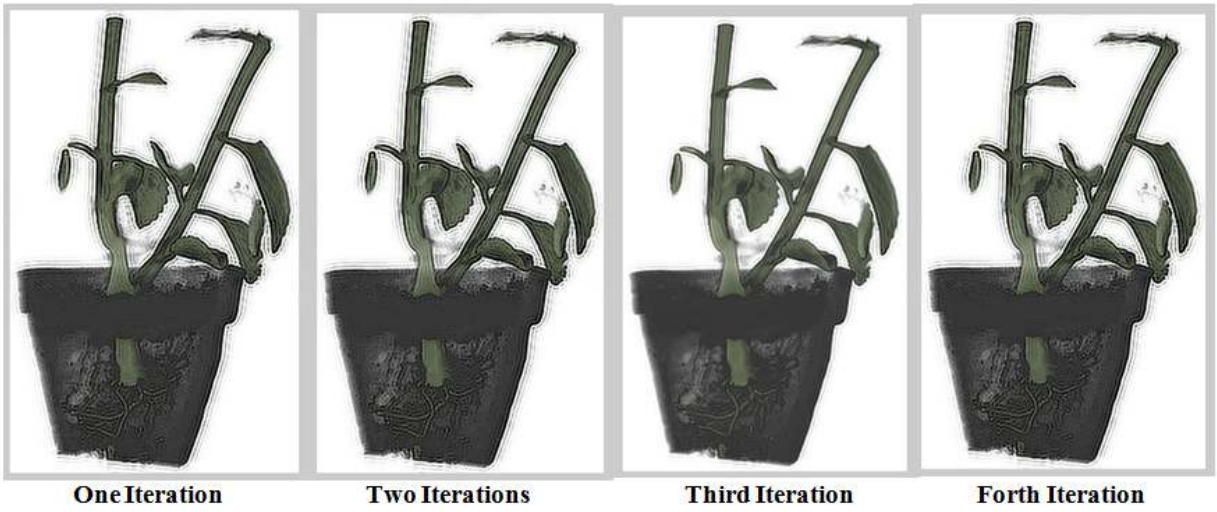

Fig. 11. Image improvement by the iteration technique.

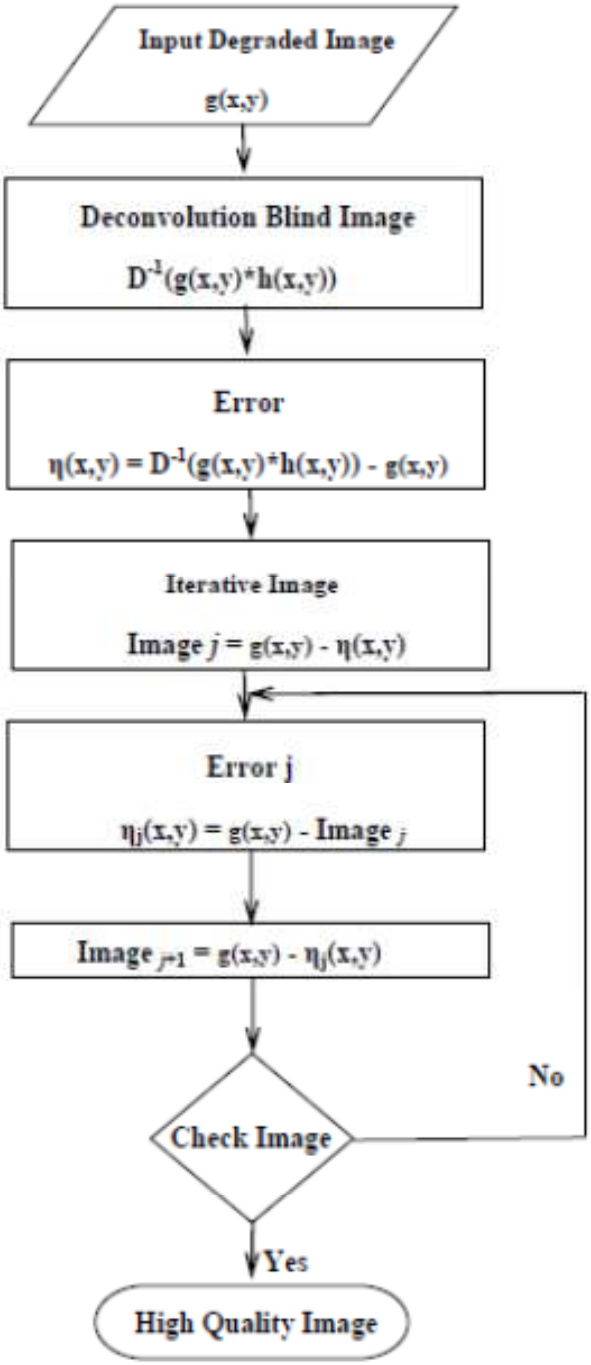

Fig. 12. Iteration technique flowchart.

The same module was executed for the CV car joint image. The results are shown in Fig. 13. The image was improvement after two iterations; i.e., less noise was appeared.

Fig. 13. Noise suppression by the iteration technique.

5. Analysis of the results:

The proposed methods aimed to improve the image quality, increase the image details, and reduce the noise by applying different digital filters. The proposed methods were based on removing the low frequency noise of the image by adjusting the cut-off frequency. Then, the low frequency Gaussian image, Butterworth image and low-pass filter images were created.

The iteration model provided high quality image by creating a blind deconvolution image that subtracted from the unprocessed image to form first iterative noise depression image. The resultant image subtracted from the NT image to form the second iterative noise depression image. The iteration technique was executed until a degree of improved image was reached. The final image has information details with error suppression. Fig. 14 shows the enhancement in the root part of the plant by the different techniques.

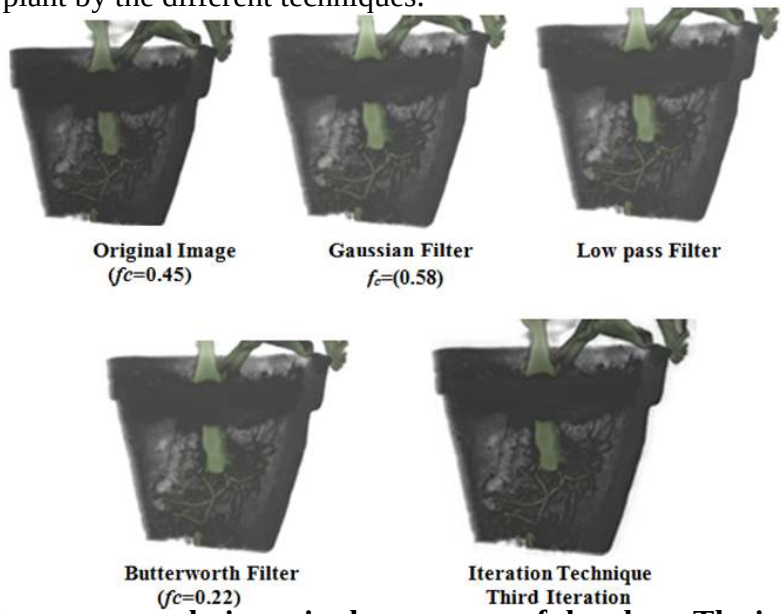

Fig. 14. Enhancement techniques in the root part of the plant. The iteration module is potentially effective.

With respect to the CV car joint image, the technique still has to be improved. The image based convolution Kernel was selected and adapted. The code was based on equation (3). The resultant second iterative deconvolved image was convolved by a selective convolution Kernel [0.01, 1 0.19]. The output denoising image is shown in Fig. 15.

Fig. 15. Enhanced denoising image by a selective deconvolution Kernel technique.

Conclusions:

The MATLAB code is a useful software package for image processing and analysis. The software implements mathematical formulas and filters for image correction and enhancement. Low-pass filters were applied in this work for improve the image. It was found that the software is a powerful tool for image enhancement.

An iteration technique module was designed to improve the image quality and reduce the noise; this resulted in increased image details in comparison with the other techniques.

Acknowledgments:

The author would like to thank the ETRR-2 operation staff for the reactor operation during the experiment. Special thanks to Waleed Ibrahim for image reconstruction by neutron tomography and Mohammed Yehya as well.

References:

[1] J. G. Walker, D. A. Fish, A. M. Brinicombe, and E. R. Pike, “Blind deconvolution by means of the Richardson–Lucy algorithm” J. Opt. Soc. Am. A, Vol. 12, No. 1, January 1995.
[2] Arijit Dutta, Aurindam Dhar, Kaustav Nandy, Project report on “Image Deconvolution By Richardson Lucy Algorithm”, Indian Statistical Institute, November, 2010.
[3] G. R. Ayers and J. C. Dainty, “Iterative blind deconvolution method and its applications,” Opt. Lett. Vol.13, pp. 547–549 , 1988.
[4] Iuri S. Bessa, et al., “Evaluation of different digital image processing software for aggregates and hot mix asphalt characterizations”, Construction and Building Materials 37, 370–378, 2012.

[5] Julien Mairal, et al., “Sparse learned representations for image restoration”, IASC, Yokohama, Japan, December 5-8, 2008.
[6] M. N. Salihin, Yusoff and A. Zakaria, “Determination of the optimum filter for qualitative and quantitative 99mTc myocardial SPECT imaging”, Iran. J. Radiat. Res., 6 (4): 173-182, 2009.
[7] Laere KV, Koole M, Lemahieu L, Dierckx R, “Image filtering in single-photon emission computed tomography: principles and applications”, Comput Med Imaging Graph, 25: 127-133, 2001.
[8] http://www.pco.de/categories/sensitive-cameras/pco2000/.
[9] Anil Gupta and Raman Kumar, “Design and Analysis of an Algorithm for Image Deblurring using Bilateral Filter”, International Journal for Science and Emerging Technologies with Latest Trends, 5(1): 28-34 (2013),
[10] Haver T.,"Introduction to signal processing-Deconvolution", University of Maryland at College Park. Retrieved 2007,
[11] Stanley Osher, et al., “An Iterative Regularization Method for Total Variation-Based Image Restoration”, Multiscale Model. Simul.1-30, 2005.
[12] Lakhwinder Kaur and Parbhjot Kaur, “Performance Evaluation of Noise Reduction Filters”, IJECT Vol. 4, 58-61, Issue Spl - 3, April - June 2013.
[13] Julien Mairal, et al., “Sparse Representation for Color Image Restoration”, IEEE Transactions on Image Processing, 53-69, Vol. 17, No. 1, Jan. 2008.
[14] F Edward Boas andDominik Fleischmann,“CT artifacts: Causes and Reduction Techniques”, Imaging Med., 4(2), 229-240, 2012.
[15] Vandenberghe S, et al.,“Iterative Reconstruction Algorithms in Nuclear Medicine. Computerized Medical Imaging and Graphics25(2), 105-111, 2001.
[16] Fleischmann D and Boas F., “Computed Tomography-Old Ideas and New Technology”, Eur. Radiol.21(3), 510-517, 2011.
[17] Martino Nicolini and Fabio Cavicchio, Astroart 5.0 user manual, http://www.msb-astroart.com/support.htm.
[18] Y. Yao, et al., “Research on the Implementation of Image Degradation and Restoration by using Model-Based Design Methodology”, International Journal of Smart Home Vol. 9, No. 9, 167-176, 2015.
[19] Aziz Makandar and Bhagirathi Halalli, “Image Enhancement Techniques using Highpass and Lowpass Filters”, International Journal of Computer Applications, Vol. 109, No. 14, 0975 – 8887, January 2015.